A Multistate-Based Control System Approach Toward Optimal Maintenance Planning

Bo Wang, Zhou Wu, and Xiaohua Xia

***Abstract*— This brief incorporates the multistate system into a control system approach to address the maintenance plan optimization (MPO) problem. The maintenance plan focuses on the totality of a set of items. A building energy efficiency retrofitting context is employed, where the retrofitted items are categorized into several homogeneous groups. The homogeneous group population dynamics and the aggregate performance dynamics under the impacts of multistate deteriorations and maintenances are formulated as a control system model. Thereafter, the MPO is cast into an optimal control problem. A model-predicative-control-based approach is employed to solve the optimal control problem with system uncertainties. A case study is conducted to illustrate the effectiveness of the present approach.**

***Index Terms*— Control system modeling, maintenance plan optimization (MPO), model predictive control (MPC), multistate system (MSS), neighborhood field optimization.**

I. Introduction

IN PRACTICE, the performances of a system can change over time due to deterioration. For example, in a building energy efficiency retrofitting project, the energy savings of the retrofitted items decrease from the design value due to deterioration. Furthermore, according to the measurement and verification (M&V) principles [1], a malfunctioning item results in the absence of its energy saving. The aggregate energy saving thereby deteriorates over time from the M&V perspective [2]. As maintenance actions can restore the energy saving of a deteriorated item, the performances of the totality of the retrofitted items manifest significant dynamics under the impacts of deterioration and maintenance. In this way, the performance dynamics, namely, maintenance dynamics, is interpreted as a control system. The maintenance plan optimization (MPO) problem is cast into an optimal control problem, where control approaches can be introduced to facilitate the maintenance planning [3], [4].

There are generally two categories of maintenance actions: preventive maintenance (PM) and corrective maintenance (CM). According to MIL-STD-721C [4], PM refers to all actions performed in an attempt to retain an item in a specified condition and CM involves the repairs and replacements against failures. Wang and Xia [4] proposed a control system interpretation of the CM plan optimization in building energy efficiency retrofitting. However, incorporating the PM into the control system framework remains unexplored. Furthermore, existing studies take into account of only malfunctions of items. The decrease in energy saving is omitted. In practice, equipment can deteriorate to a worse working state before malfunctions, e.g., air conditioners and heat pumps consume more energy upon usage. Such a relationship has been revealed [5], [6], and existing studies lack relative discussions.

In reliability engineering, the multistate system (MSS) is able to characterize the multiple performance levels of a system [7]. The MSS is usually defined as a multiworking and failure-state system that has a range of performance levels, from perfectly functioning to complete failure, resulting from the deterioration and failure of some components in the system [8]. In the scope of the MSS model, CM represents the actions that restore the system from a failure state and the PM actions are carried out before failures, restoring the system to a better state. According to [9], existing efforts focus on the maintenance planning of one deteriorating system with multiple working states. The state transition of the system is considered to be governed by a Markov process in some relevant studies [10], where the system state is described as a set of probabilities corresponding to the working states. In the building context, the state of the totality of retrofitted items can become very complicated as the aggregate performances are influenced by various categories of retrofitted items that are corresponding to different performance levels. Therefore, the retrofitted items are categorized into several homogeneous groups for simplicity. A hypothesis is made to obtain the categorization: items from the same homogeneous group have the same inherent energy and reliability performances, the same operating schedules, and a similar operational environment. Such items have the same energy savings and can be characterized by the same MSS model. Practically, this assumption is easy to implement such that lighting is grouped according to installations in offices, public areas, and board rooms [3]. The general theoretical robustness of this hypothesis in practice yet remains an open problem that requires further exploration. An arbitrary homogeneous group can be further divided into several subsets according to the item working state. We specially employ the term population to represent the count of items within a homogeneous group under a specific working state. The populations of the subsets are commensurate with the probabilities of an individual item manifesting different working states. The population dynamics thereby represents the process that a number of items transit from one working state to another, resulting in the changes of populations of corresponding subsets. Such population changes are

Manuscript received September 21, 2015; revised February 18, 2016; accepted March 12, 2016. Date of publication April 27, 2016; date of current version December 14, 2016. Manuscript received in final form March 28, 2016. Recommended by Associate Editor D. Vrabie.

B. Wang and X. Xia are with the Department of Electrical, Electronic and Computer Engineering, University of Pretoria, Pretoria 0028, South Africa (e-mail: wb8517@gmail.com; xxia@up.ac.za).

Z. Wu was with the University of Pretoria, Pretoria 0028, South Africa. He is now with the School of Automation, Chongqing University, Chongqing 400044, China (e-mail: wuzhsky@gmail.com).

Color versions of one or more of the figures in this paper are available online at http://ieeexplore.ieee.org.

Digital Object Identifier 10.1109/TCST.2016.2550505

commensurate with the state transition probabilities of an individual item.

Thereafter, the population dynamics can be modeled as a control system. In this way, the MPO problem is cast into an optimal control problem, where the control approaches can be introduced, e.g., the model predictive control (MPC). The MPC finds the optimal control inputs by predicting the future based on the present state of the system. In [11] and [12], the MPC algorithm convergence and the robustness against disturbances in controller implementation or state measurement have been investigated and verified for a kind of constrained minimization problem over a receding finite horizon. It is noted that the theoretical proof of such stability and robustness of MPC exists only in a few circumstances [13], rarely in the case of discrete variable MPC [14]. The MPC approach is employed for the MPO problem. The MPC algorithm design is extensively explored in the past decades to suit complicated requirements [15]. At the current stage, the control objective from [4] is employed, which is a weighted sum of two optimization objectives: maximizing the aggregate energy saving and maximizing the internal rate of return (IRR) [16] for a retrofitting project over a predecided finite-time period, namely, the sustainability period. Some constraints over a whole finite horizon, e.g., the targeted energy saving and the budget limit, can be involved in the MPO optimal control problem. Therefore, the employed MPC algorithm is modified to take into account the history performances. In practice, the state variables and control inputs are both integers as they represent the counts of items, and the IRR is a nonanalytic performance indicator. Consequently, an improved differential evolutionary (DE) algorithm with a binary neighborhood field optimization (BNFO) method [17] is employed as a numerical solver.

The main contribution of this brief is a multistate-based control system approach for the MPO problem taking into account different levels of deteriorations and impacts of both PM and CM actions. An alternative MSS model is employed to describe the states of a set of homogeneous items, and a state-space model is formulated based on the alternative MSS model. The state variables are the populations of the item subsets corresponding to different working states. For simplicity, assuming the PM actions restores a specific amount of items from the worse state to the best state and the CM actions from the malfunctioning state to the best state. We adopt the term maintenance intensity to describe the count of items being restored by the maintenance actions. The control inputs are the maintenance intensities. The maintenance time schedule, i.e., the instants when maintenance actions are applied, is assumed fixed and known *a priori*. Installing additional equipment other than the retrofitted item group is ignored at the current stage, and therefore, the system states are physically bounded. The system uncertainties are also taken into account. The MPC controller is designed and a DE-algorithm-based numerical solver is employed. A building energy efficient retrofitting project is adopted as the case study to test and verify the effectiveness of the proposed approach.

The remainder of this brief consists of four sections. Section II gives the control system framework and the state-space model formulation. Section III introduces the optimal control problem formulation, the MPC controller design, and the numerical solver. Section IV provides the simulation results and analysis. Section V draws conclusions.

II. Control System Modeling

A. Control System Framework for MPO Problem

Let $t_k = kS$, $k = 0, 1, 2, \ldots$ denote the sampling instants during operation, where S indicates the sampling interval. An MPO problem with finite decision horizon $k = \{0, 1, 2, \ldots, T\}$ is introduced. This finite decision horizon indicates a collection of sampling instants over the sustainability period [0, TS). Given a homogeneous group l with N_l items and M_l different working states corresponding to the different performance levels. Let $G_l(t_k)$ denote the performance level of an arbitrary item at instant t_k. $G_l(t_k)$ takes value from the set

$$\mathbf{g}_l = \{g_{l,1}, g_{l,2}, \ldots, g_{l,M_l}\} \tag{1}$$

and working state i corresponds to the performance level $g_{l,i}$. $\mathbf{g}_l$ is given in ascending order, where g_{l,M_l} denotes the maximum energy saving an item can contribute under the best working state and $g_{l,1}$ denotes the minimum saving under the worst state. Accordingly, the homogeneous group l can be divided into M_l subsets corresponding to different working states, i.e., $\forall i \in [1, M_l]$, subset i consists of all items from group l that are under working state i, i.e., subject to $G_l(t_k) = g_{l,i}$. The subset populations are dynamic. Let $\mathbf{x}_l(t_k)$ denote the populations of all subsets in group l at t_k

$$\mathbf{x}_l(t_k) = [x_{l,1}(t_k), x_{l,2}(t_k), \ldots, x_{l,M_l}(t_k)]^T \tag{2}$$

where $x_{l,i}(t_k)$ denotes the population of subset i at instant t_k, $\sum_{i=1}^{M_l} x_{l,i}(t_k) = N_l$. Let $\mathbf{u}_l(t_k)$ denote the maintenance intensities for group l during $[t_k, t_{k+1})$

$$\mathbf{u}_l(t_k) = \left[u_1^l(t_k), u_2^l(t_k), \ldots, u_{M_l-1}^l(t_k), u_C^l(t_k)\right]^T \tag{3}$$

where $u_i^l(t_k)$ denotes the PM intensities, i.e., the count of items under state i and restored to state M_l. $u_C^l(t_k)$ denotes the CM intensities, i.e., the count of malfunctioning items that are restored to state M_l. In practice, the numbers of items are integers, and therefore, $x_{l,i}(t_k)$, $u_i^l(t_k)$, and $u_C^l(t_k)$ are integers accordingly. Given predecided PM time schedule P and CM time schedule Q, where $P = \{m_1^p, m_2^p, \ldots, m_{T_p}^p\}$ and $Q = \{m_1^c, m_2^c, \ldots, m_{T_c}^c\}$, respectively, denote a set of indices of sampling instants, namely, the maintenance instants. The elements of P and Q are selected from $k = 0, 1, 2, \ldots, T$, implying that the maintenance instants are commensurate with the sampling instants t_k. For t_k with $k \notin P$, $u_i^l(t_k) = 0$ with $\forall i \in [1, M_l]$. For t_k with $k \notin Q$, $u_C^l(t_k) = 0$.

Given $\bar{N}$ homogeneous groups in the MPO problem, let $\mathbf{x}(t_k) = [\mathbf{x}_1(t_k), \mathbf{x}_2(t_k), \ldots, \mathbf{x}_{\bar{N}}(t_k)]^T$ denote the *state variable vector*, $\mathbf{u}(t_k) = [\mathbf{u}_1(t_k), \mathbf{u}_2(t_k), \ldots, \mathbf{u}_{\bar{N}}(t_k)]^T$ the *control input vector*, and $F_l(\mathbf{x}_l(t_k), \mathbf{u}_l(t_k))$ the population changes in group l under the impacts of deteriorations and maintenances. A compact form of the state-space model can be obtained as

$$\begin{bmatrix} \mathbf{x}_1(t_{k+1}) \\ \vdots \\ \mathbf{x}_{\bar{N}}(t_{k+1}) \end{bmatrix} = \begin{bmatrix} \mathbf{x}_1(t_k) \\ \vdots \\ \mathbf{x}_{\bar{N}}(t_k) \end{bmatrix} + \begin{bmatrix} D_1(\mathbf{x}_1(t_k), \mathbf{u}_1(t_k)) \\ \vdots \\ D_{\bar{N}}(\mathbf{x}_{\bar{N}}(t_k), \mathbf{u}_{\bar{N}}(t_k)) \end{bmatrix} \tag{4}$$

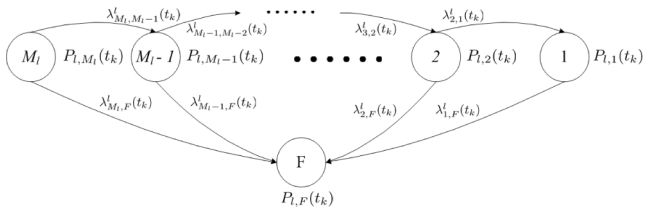

Fig. 1. State transition diagram of an individual item from homogeneous group l with M_l working states and one malfunctioning state.

where

$$D_l(\mathbf{x}_l(t_k), \mathbf{u}_l(t_k)) = [\triangle x_{l,M_l}(t_k), \triangle x_{l,M_l-1}(t_k), \ldots, \triangle x_{l,1}(t_k)]^T \quad (5)$$

with $\triangle x_{l,i}(t_k)$ representing the population change of subset i in group l. The initial state is $\mathbf{x}(t_0) = \mathbf{x}_0 = [\mathbf{x}_1^0, \mathbf{x}_2^0, \ldots, \mathbf{x}_{\bar{N}}^0]^T$.

B. Population Change Formulation

In homogeneous group l, $x_{l,i}(t_k)$ changes over each sampling interval. The state transition of an individual item from group l is demonstrated in Fig. 1, where $P_{l,i}(t_k)$, $i \in [1, M_l]$ denotes the probability that this item works under state i and performance level $g_{l,i}$. $\lambda_{i,i-1}^l(t_k)$ indicates the state transition from state i to state $i-1$ over the sampling interval $[t_k, t_{k+1})$. The circle F denotes the malfunctioning state and $P_{l,F}(t_k)$ the probability of this item being malfunctioning. $\lambda_{i,F}^l(t_k)$ indicates the state transition from state i to malfunctioning. As shown in Fig. 1, $P_{l,i}(t_k)$ increases due to transition $\lambda_{i+1,i}^l(t_k)$ and decreases due to transition $\lambda_{i,i-1}^l(t_k)$ and transition $\lambda_{i,F}^l(t_k)$ simultaneously. $P_{l,M_l}(t_k)$ continuously decreases and $P_{l,F}(t_k)$ continuously increases without maintenance. Boukas and Liu [10] formulate such a state transition as a Markov process. As introduced in the previous section, the population dynamics of homogeneous group l is commensurate with the individual item state transition. Taking advantage of the Makrov process formulation in [10], the population changes $D_l(\mathbf{x}_l(t_k), \mathbf{u}_l(t_k))$ in group l are formulated in (6), as shown at the bottom of this page, where $f_{i,i-1}^l(\mathbf{x}_{l,i}(t_k))$ denote the population change from subset i to subset $i-1$ that is resulted from the transition $\lambda_{i,i-1}^l(t_k)$.

Please note that (6) describes a simplified state transition process, assuming that transition exists only between a pair of neighbor states or from current state to malfunctioning state. $f_{i,i-1}^l(\mathbf{x}_{l,i}(t_k))$ can be obtained via the deterioration model by experimental data fitting, e.g., Carstens *et al.* [18] obtain a model characterizing the decay of the compact fluorescent lamp populations over time. It is expected that the employment of such empirical models can facilitate the population dynamics modeling. Some other deterioration models can be found from the reliability studies [19].

Several assumptions are made to allow (6) as follows.

1) The maintenance downtime and degradations of the maintained items at t_k are ignored over $[t_k, t_{k+1})$.
2) The state transition intensities of the items are known *a priori* by the planner.
3) The working states of the retrofitted items can be perceived. The inspections at t_k are considered as the actual populations during $[t_{k-1})$.

III. Controller Design

A. Objective Function Formulation

The aforementioned maintenance planning for a building retrofitting project is employed to demonstrate the applicability of our approach. In a building retrofitting project, we categorize the retrofitted items into two types. The type-I retrofitted items undertake no PM over the life cycle. After the breakdown of a type-I item, corrective replacement takes place and the failed item is scrapped. Energy efficient globes and motion sensors are typical type-I items. The energy saving degradation of the type-I retrofits are not taken into account at the current stage. The type-II retrofitted items are more complicated. The performance levels of a type-II item are indicated by the estimated energy savings, computed following the M&V principles [1]. A type-II item can deteriorate to a worse working state before becoming malfunctioning. The PM actions are introduced to restore the type-II item to a better state. The CM actions also take place to address the malfunctions. Air conditioners and heat pumps are typical type-II items. Given the type-I item, a special case of the MSS (2) applies to both item types.

There are two objectives: the energy saving amount and the IRR. The constraints include the targeted energy saving amount limit, the budget limit, and the payback period limit. Given a series of performance characteristics that is obtained via preimplementation audit and simulation

$$\begin{cases} \mathbf{a}_l(t_k) = \{a_{l,1}(t_k), a_{l,2}(t_k), \ldots, a_{l,M_l}(t_k)\} \\ \mathbf{b}_l(t_k) = \{b_{l,1}(t_k), b_{l,2}(t_k), \ldots, b_{l,M_l}(t_k)\} \\ \mathbf{C}_l(t_k) = \left\{C_1^l(t_k), C_2^l(t_k), \ldots, C_{M_l}^l(t_k), C_C^l(t_k)\right\} \end{cases} \quad (7)$$

where $\mathbf{a}_l(t_k)$ denotes the average energy saving over the sampling interval $[t_{k-1}, t_k)$ and $\mathbf{b}_l(t_k)$ the average cost saving. $\mathbf{C}_l(t_k)$ denotes the maintenance cost. In (7), for $i \in [1, M_l]$,

$$\begin{cases} \triangle x_{l,M_l}(t_k) = -f_{M_l,M_l-1}^l(\mathbf{x}_{l,M_l}(t_k)) - f_{M_l,F}^l(\mathbf{x}_{l,M_l}(t_k)) + \sum_{i=1}^{M_l-1} u_i^l(t_k) + u_C^l(t_k) \\ \triangle x_{l,M_l-1}(t_k) = f_{M_l,M_l-1}^l(\mathbf{x}_{l,M_l}(t_k)) - f_{M_l-1,Ml-2}^l(\mathbf{x}_{l,M_l-1}(t_k)) - f_{M_l-1,F}^l(\mathbf{x}_{l,M_l-1}(t_k)) - u_{M_l-1}^l(t_k) \\ \vdots \\ \triangle x_{l,2}(t_k) = f_{3,2}^l(\mathbf{x}_{l,3}(t_k)) - f_{2,1}^l(\mathbf{x}_{l,2}(t_k)) - f_{2,F}^l(\mathbf{x}_{l,2}(t_k)) - u_2^l(t_k) \\ \triangle x_{l,1}(t_k) = f_{2,1}^l(\mathbf{x}_{l,2}(t_k)) - f_{1,F}^l(\mathbf{x}_{l,1}(t_k)) - u_{1,M_l}^l(t_k) \end{cases} \quad (6)$$

$a_{l,i}(t_k)$ and $b_{l,i}(t_k)$ denote the performance characteristics corresponding to an individual item with $G_l(t_k) = g_{l,i}$. $C_i^l(t_k)$ denote the PM cost and $C_C^l(t_k)$ the CM cost. Thereafter, the aggregate energy savings can be formulated as

$$\begin{cases} \mathrm{ES}(t_k) = \sum_{l=1}^{\bar{N}} \sum_{i=1}^{M_l} a_{l,i}(t_k) x_{l,i}(t_k) \\ \mathrm{ES}|_{\mathrm{all}} = \sum_{k=1}^{T} \mathrm{ES}(t_k) \end{cases} \tag{8}$$

and the corresponding cost savings are

$$\begin{cases} B(t_k) = \sum_{l=1}^{\bar{N}} \sum_{i=1}^{M_l} b_{l,i}(t_k) x_{l,i}(t_k) \\ B|_{\mathrm{all}} = \sum_{k=1}^{T} B(t_k) \end{cases} \tag{9}$$

the aggregate maintenance cost at each time instant is

$$h(t_k) = \sum_{l=1}^{\bar{N}} \left(\sum_{i=1}^{M_l} C_i^l(t_k) u_i^l(t_k) + C_C^l(t_k) u_C^l(t_k) \right) \tag{10}$$

and the total investment of the retrofitting project is

$$h|_{\mathrm{all}} = h_0 + \sum_{k=1}^{T} h(t_k) \tag{11}$$

where h_0 denotes the initial expenditure of implementing the retrofitting project. With the aforementioned cost savings and maintenance costs, the net present value (NPV) [16] is employed as one of the performance indicators. The NPV of the project over [0, TS) is formulated as follows:

$$\mathrm{NPV} = \sum_{k=1}^{T} \frac{B(t_k) - h(t_k)}{(1+R)^{n-1}} - h_0 \tag{12}$$

where R denotes the discount rate for NPV calculation. $n = 1, 2, \ldots$ indicates that the sampling instant t_k lies within the nth year after the implementation of the retrofitting project. However, choosing proper discount rate can be very tricky. The IRR instead of NPV is hereby employed to evaluate the economy of the project. IRR, denoted by R_T in the present model, refers to the discount rate that makes NPV = 0 over [0, TS). Usually, the investors are more desirable to undertake the project with higher IRR, and therefore, maximizing IRR becomes one of the optimization objectives.

B. Optimal Control Problem Formulation

Given the initial state $\mathbf{x}(t_0) = \mathbf{x}_0$, the predecided PM time schedule $P = \{m_1^p, m_2^p, \ldots, m_{T_p}^p\}$, and the CM time schedule $Q = \{m_1^c, m_2^c, \ldots, m_{T_c}^c\}$. The optimal control problem is to find a control law, i.e., the maintenance plan $\mathbf{u}(\cdot) = \{\mathbf{u}(t_1), \mathbf{u}(t_2), \ldots, \mathbf{u}(t_T)\}$, which minimizes the following performance index over the sustainability period:

$$J(\mathbf{x}_0, \mathbf{u}(\cdot)) = -\omega_1 \frac{\mathrm{ES}|_{\mathrm{all}}}{\alpha} - \omega_2 R_T \tag{13}$$

subject to (4)–(6), and

$$\begin{cases} \mathrm{ES}|_{\mathrm{all}} \geq \alpha \\ \sum_{k=1}^{T} h(t_k) \leq \beta \\ \mathrm{NPV}|_0^{T_{\mathrm{pp}}} \geq 0 \\ \mathbf{0} \leq \mathbf{x}(t_k) \leq \mathbf{x}_0 \end{cases} \tag{14}$$

where ω_1 and ω_2 denote the weighting factors. α denotes the target energy saving amount and β the maintenance budget limit over [0, TS). T_{pp} represents the maximum acceptable payback period and $\mathrm{NPV}|_0^{T_{\mathrm{pp}}}$ denotes the NPV computed over $[0, T_{\mathrm{pp}}S)$.

C. MPC Controller

An MPC-based approach is employed to solve the optimal control problem in (13) and (14). In existing studies, the MPC prediction horizon can be time varying [20]. Given some constraints in (14) involve the performance index over the whole sustainability period, then a decreasing horizon mechanism is implemented. The predictive horizon at instant t_m covers the rest of the sustainability period, i.e., the horizon $N = T - m$. A mathematical transformation of the optimal control problem is accordingly applied, where the open-loop problem over $[t_m, \mathrm{TS})$ is defined as a dynamic programming problem that minimizes the following performance index:

$$J'(\mathbf{x}(t_m), \mathbf{u}'|_m(\cdot)) = -\omega_1 \frac{\mathrm{ES}'|_m}{\alpha} - \omega_2 R_T' \tag{15}$$

where R_T' is the discount rate that makes $\mathrm{NPV}'|_m = 0$, with

$$\begin{cases} \mathrm{ES}'|_m = \sum_{k=1}^{m} \bar{\mathrm{ES}}(t_k) + \sum_{k=m+1}^{T} \mathrm{ES}(t_k) \\ \mathrm{NPV}'|_m = \sum_{k=1}^{m} \frac{\bar{B}(t_k) - \bar{h}(t_k)}{(1+R)^{n-1}} + \sum_{k=m+1}^{T} \frac{B(t_k) - h(t_k)}{(1+R)^{n-1}} - h_0 \end{cases} \tag{16}$$

subject to (4)–(6), and

$$\begin{cases} \mathrm{ES}'|_m \geq \alpha \\ h'|_m \leq \beta', \quad m \in R \\ \mathrm{NPV}'|_m^{T_{\mathrm{pp}}} \geq 0 \\ \mathbf{0} \leq \mathbf{x}(t_m) \leq \mathbf{x}_0 \end{cases} \tag{17}$$

where

$$\begin{cases} h'|_m = \sum_{k=m+1}^{T} h(t_k) \\ \beta' = \beta - \sum_{k=1}^{m} \bar{h}(t_k) \\ \mathrm{NPV}'|_m^{T_{\mathrm{pp}}} = \sum_{k=1}^{m} \frac{\bar{B}(t_k) - \bar{h}(t_k)}{(1+R)^{n-1}} + \sum_{k=m+1}^{T_p} \frac{B(t_k) - h(t_k)}{(1+R)^{n-1}} - h_0. \end{cases} \tag{18}$$

$\bar{\mathrm{ES}}(t_k)$, $\bar{B}(t_k)$, and $\bar{h}(t_k)$, respectively, denote the energy saving, the cost saving, and the maintenance cost in history, respectively, i.e., the existing performance measures resulting from the executed control inputs. Consequently, the problem

in (15)–(18) is solved over the interval $[t_m, \mathrm{TS})$ when $m \in P$ or $m \in Q$, and a series of optimal control rates is obtained, represented by $\mathbf{u}'|_m = \{\mathbf{u}'(t_k) : k = m, m+1, \ldots, T-1\}$. Only the optimal solution in the first sampling period $[t_m, t_{m+1})$ is applied, represented by $\bar{\mathbf{u}}|_m = \{\mathbf{u}'|_m(t_m)\} = \{\bar{\mathbf{u}}|_m(\mathbf{x}(t_m))\}$, where the last equation is to emphasize the functional dependence of the optimal control on the initial state $\mathbf{x}(t_m)$ of the MPC formulation in (15)–(18). According to (4), $\bar{\mathbf{u}}|_m$ is applied and $\mathbf{x}(t_{m+1})$ is thus obtained. $\mathbf{x}(t_{m+1})$ then becomes the initial condition of the MPC formulation over the time horizon $[t_{m+1}, \mathrm{TS})$. These are taking place consecutively over the sustainability period to obtain the optimal control inputs $\bar{\mathbf{u}}$.

In practice, uncertainties can influence the prediction of state variables. Let $\mathbf{d}(t_k) = [\mathbf{d}_1(t_k), \mathbf{d}_2(t_k), \ldots, \mathbf{d}_{\bar{N}}(t_k)]^T$ denote the impacts of uncertainties, the actual state $\hat{\mathbf{x}}(t_{m+1}) = \mathbf{x}(t_{m+1}) + \mathbf{d}(t_k)$, which can be measured through inspections. The actual state is utilized to be the initial condition of prediction horizon $[t_{m+1}, \mathrm{TS})$. In the MPO problem, the system states are physically bounded. The stability of such a closed-loop system has been investigated in [21].

MPC Algorithm (Initialization): Let initial state $\mathbf{x}(t_0) = \mathbf{x}_0$ and $m = 0$.

1) Compute the open-loop optimal solution $\{\mathbf{u}'|_m(t_k)\}$ of the problem formulation (15)–(18), where $k = m, m+1, \ldots, T-1$.
2) The MPC controller $\bar{\mathbf{u}}|_m = \{\mathbf{u}'|_m(t_m)\}$ is applied after the sampling instant t_m. The remains of the open-loop optimal solution $\{\mathbf{u}'|_m(t_k) : k = m+1, \ldots, T-1\}$ are discarded. The predicted $\mathbf{x}(t_{m+1})$ are then obtained according to (4)–(6). As a result of the uncertainties, the actual system state over the next sampling period is updated according to
$$\begin{bmatrix} \hat{\mathbf{x}}_1(t_{m+1}) \\ \vdots \\ \hat{\mathbf{x}}_{\bar{N}}(t_{m+1}) \end{bmatrix} = \begin{bmatrix} \mathbf{x}_1(t_{m+1}) \\ \vdots \\ \mathbf{x}_{\bar{N}}(t_{m+1}) \end{bmatrix} + \begin{bmatrix} \mathbf{d}_1(t_m) \\ \vdots \\ \mathbf{d}_{\bar{N}}(t_m) \end{bmatrix}$$
which is inspected at t_{m+1} and executed over $[t_m, t_{m+1})$.
3) Let $\hat{\mathbf{x}}(t_{m+1}) = \{\hat{\mathbf{x}}_1(t_{m+1}), \ldots, \hat{\mathbf{x}}_{\bar{N}}(t_{m+1})\}$ be the initial state for the next predictive horizon, $m := m+1$ and go back to step 1).

According to the predecided maintenance time schedules P and Q, $\mathbf{u}(t_m) = 0$ when $m \notin P$ and $m \notin Q$, where step 1) is skipped and $\hat{\mathbf{x}}(t_{m+1})$ is obtained by
$$\begin{bmatrix} \hat{\mathbf{x}}_1(t_{m+1}) \\ \vdots \\ \hat{\mathbf{x}}_{\bar{N}}(t_{m+1}) \end{bmatrix} = \begin{bmatrix} \mathbf{x}_1(t_m) \\ \vdots \\ \mathbf{x}_{\bar{N}}(t_m) \end{bmatrix} + \begin{bmatrix} D_1(\mathbf{x}_1(t_m), 0) \\ \vdots \\ D_{\bar{N}}(\mathbf{x}_{\bar{N}}(t_m), 0) \end{bmatrix} + \begin{bmatrix} \mathbf{d}_1(t_m) \\ \vdots \\ \mathbf{d}_{\bar{N}}(t_m) \end{bmatrix}.$$
The above MPC algorithm will go over the sustainability period to solve out the optimal control strategy.

D. DE-Based Numerical Solver

To most nonlinear optimization problems, the DE algorithm can hopefully, although not guaranteed, discover a satisfactory solution after sufficient iterations, where the nonlinearity can be addressed with easier computer implementation [22].

Algorithm 1 Pseudocode of DE Algorithm With BNFO Method

Definition:
np: the population size;
d: dimension of the problem;
X: the decision matrix with the size of np*d;
J: the function value vector with the size of np*1;
Mg: the maximum number of generations for stopping criterion.

BEGIN
Set mutation probability C_r and learning rate α;
Create a random, binary coded initial population $\{x_{i,1} | i = 1, 2, ..., np\}$;
Let $x_{best} = x_{1,1}$;
while $G = 1$ *to* Mg **do**
  while $i = 1$ *to* np **do**
    Locate $x_{i,G}$ in X and obtain its superior neighbor $xc_{i,G}$ and inferior neighbor $xw_{i,G}$;
    $\alpha_{r1} = rand < \alpha$; $\alpha_{r2} = rand < \alpha$;
    $v_1 = \alpha_{r1}$ & $xor(x_{i,G}, xc_{i,G})$;
    $v_2 = \alpha_{r2}$ & $xor(xw_{i,G}, xc_{i,G})$;
    $v_{i,G} = xor(x_{i,G},\ v_1|v_2)$;
    Repair $v_{i,G}$ if it violates the upperbound or lowerbound;
    Generate $j_{rand} = randint(1, d)$;
    while $j = 1$ *to* d **do**
      if $j = j_{rand}$ or $rand(0,1) < CR$ **then**
        $u_{j,i,G} = v_{j,i,G}$;
      else
        $u_{j,i,G} = x_{j,i,G}$;
      end if
    end while
    if $J(u_{i,G}) \le J(x_{i,G})$ **then**
      $x_{i,G+1} = u_{i,G}$;
      if $J(x_{i,G+1}) < J(x_{best})$ **then** $x_{best} = x_{i,G+1}$;
      end if
    else
      $x_{i,G+1} = x_{i,G}$;
    end if
  end while
end while
Return x_{best};
END

Wang and Xia [4] employ the DE algorithm as a numerical solver to the optimal CM planning problem.

Given R'_T a nonanalytic performance index formulation and $\mathbf{x}$ and $\mathbf{u}$ of (13) and (14) integers as mentioned earlier, then the dynamic programming problem (15)–(18) is a nonlinear integer optimization problem. An improved DE algorithm with the the BNFO method is thereby employed as the numerical solver to (15)–(18). The idea of the BNFO method comes from the biological world, where individuals often communicate with and learn from their neighbors within a limited perceptual range. Similarly, the individuals in BNFO method are mostly affected by the local environment rather than the global one, i.e., each individual is updated under the concept of learning from the neighbors, that is, following superior neighbors and diverging from inferior neighbors [23]. The utilization of the attractive field of the superior neighbor and the repulsive field of the inferior neighbor in the BNFO method is able to deliver promising results efficiently within acceptable computational time, thereby reducing the computational cost [24]. As a solver to the integer optimization problem, the sequences of bits are employed to represent the individuals in the BNFO method. The pseudocode of the DE algorithm with the BNFO method is given in Algorithm 1. More details of the BNFO can be

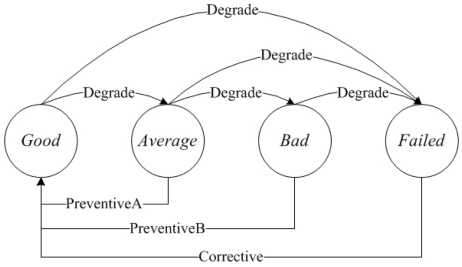

Fig. 2. State transition diagram for type-II items in the case study.

TABLE I
TRANSITION INTENSITIES OF INVOLVED RETROFITS (IN MONTHS)

Retrofitted Items	Type	MTBF	t1 (good to average)	t2 (average to bad)
Motion sensor	I	33.5	N/A	N/A
20W retrofit LED	I	27.2	N/A	N/A
180W new projector	I	32.8	N/A	N/A
3kW heat-pumps	II	52	25.2	100
New air conditioner	II	43.8	21.6	86.4

found in [17] and [24], where the comparison with other stochastic optimization approaches, e.g., the genetic algorithm, the particle swarm optimization, is discussed thoroughly.

Remark 1: In general, the DE improved algorithm manifests satisfying performances compared with other stochastic optimization approaches. As detailed analysis and comparison are not the focuses of this brief, thorough investigations can be found in [17] and [24].

IV. SIMULATION AND VERIFICATION

A small retrofitting project for a government office building is presented as our case study to verify the effectiveness of the present model. The sampling interval is 1 month and the sustainability period is 10 years, i.e., 120 months. The retrofitting plan is *a priori* decided, based on which the maintenance plan is optimized. There are five homogeneous groups of retrofitted items listed in Table II. Three of them are type-I items, including the motion sensors, the 20-W light emitting diode (LED) bulbs, and the 180-W new projectors. The 3-kW heat pumps and new air conditioners are type-II items. The type-II items have three working states, good, average, and bad, and one failure state, corresponding to different energy performance levels. The state transition diagram is illustrated in Fig. 2, where preventiveA indicates the PM action that restores the item state from average to good, preventiveB the one that restores from bad to good, and corrective the one that restores from failed to good. The type-I items switch between the good and failed states.

In our case study, the population changes are estimated by an exponential decay model from reliability engineering [19]. Let $\theta^l_{i,i-1}$ denote the transition intensity from state i to state $i-1$ for an item from homogeneous group l, and $k^l_{i,i-1} = 1/\theta^l_{i,i-1}$. The corresponding population change $f^l_{i,i-1}(\mathbf{x}_{l,i}(t_k))$ is

$$f^l_{i,i-1}(\mathbf{x}_{l,i}(t_k)) = k^l_{i,i-1} x_{l,i}(t_k). \tag{19}$$

The transition intensities are known *a priori* and illustrated in Table I, where mean time between failure (MTBF) indicates

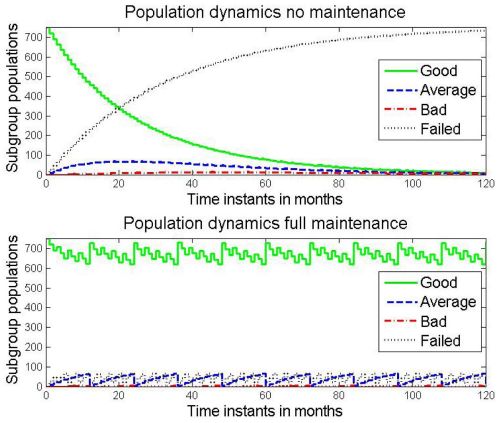

Fig. 3. Population dynamics of no maintenance and full maintenance.

the transition intensity for an item from an arbitrary working state to failure state, $t1$ indicates the one from good to average, and $t2$ indicates the one from average to bad.

In Table II, the quantities represent the initial populations of the homogeneous groups. At the initial stage, all items are in good condition. The unit prices represent the initial investment taking into account all the purchase and installation. The unit energy savings and cost savings are the monthly average measures. During the sustainability period, these saving amounts are considered constant. The preventiveA cost, preventiveB cost, and corrective cost hereby represent the average costs of implementing the respective maintenance actions.

The targeted energy saving amount is 9 067 921.6 kWh. The expenditure of implementing this retrofitting project at the initial stage is U.S. $270 760. The maintenance budget limit is U.S. $165 000 over the 120 months. The discount rate for NPV calculation is 9% per year, and the desired payback period is 40 months. An inspection will be applied at the end of each month to monitor the status of the retrofitted items, i.e., the sampling instants. The PM time schedule $P = \{11, 23, 35, 47, \ldots, 119\}$ and the CM time schedule $Q = \{2, 5, 8, 11, \ldots, 119\}$. Fig. 3 illustrates the population dynamics without maintenance and under full maintenance policy. The curves, respectively, represent the population dynamics of items under good, average, bad, and failed states from all the five categories.

Table III illustrates the solutions in five different maintenance cases: no maintenance and full maintenance where uncertainties are not included, and three optimal maintenance cases with uncertainties, namely, the optimal balance case, the energy prior case, and the economy prior case, where our method is employed. Different weighting factors are employed in these cases. For the optimal balance case, $\omega_1 = 0.5$ and $\omega_2 = 0.5$, where the two objectives are equally considered; for the energy prior case, $\omega_1 = 1.0$ and $\omega_2 = 0$, where only the energy savings are considered; for the economy prior case, $\omega_1 = 0$ and $\omega_2 = 1.0$, where only the financial payback is considered. In the latter two cases, the MPO problem is interpreted into a constrained single-objective optimization problem. The solution without maintenance illustrates the impact of the deterioration. The solution from full maintenance policy is introduced for comparison, where all the degraded

TABLE II

CHARACTERISTICS OF INVOLVED RETROFITTED FACILITIES

Retrofitted Items	Type	Quantities	Unit Energy Saving (kWh)	Unit Cost Saving ($)	Corrective Cost ($)	PreventiveA Cost ($)	PreventiveB Cost ($)
Motion sensor	I	125	95.08	11.26	196	N/A	N/A
20W retrofit LED	I	382	8.5	0.91	14.19	N/A	N/A
23 inch LCD Monitor	I	48	19.2	2.16	263.28	N/A	N/A
3kW Heat-pumps	II	86	720	81.11	201	47	65
New air conditioner	II	111	148.5	16.3	175	26	35

TABLE III

PERFORMANCE CHARACTERISTICS OF THE OBTAINED MAINTENANCE PLAN IN DIFFERENT CASES

Cases	Energy savings (kWh)	Percentage saved	IRR	Payback period (months)	NPV ($)	Maintenance cost ($)	Total investment ($)
No maintenance	3517093	38.70%	13.62%	62.77	33277.99	0	270758
Full maintenance	10687010	117.86%	33.18%	40.62	338954.1	255249.6	526007.6
Optimal Balance	10367170	114.31%	35.06%	39.33	366320.5	164992.1	435750.1
Energy Prior	10381420	114.49%	34.92%	39.32	366461.8	164989.6	435747.6
Economy Prior	10256830	113.11%	35.23%	39.34	364942	156841.6	427599.6

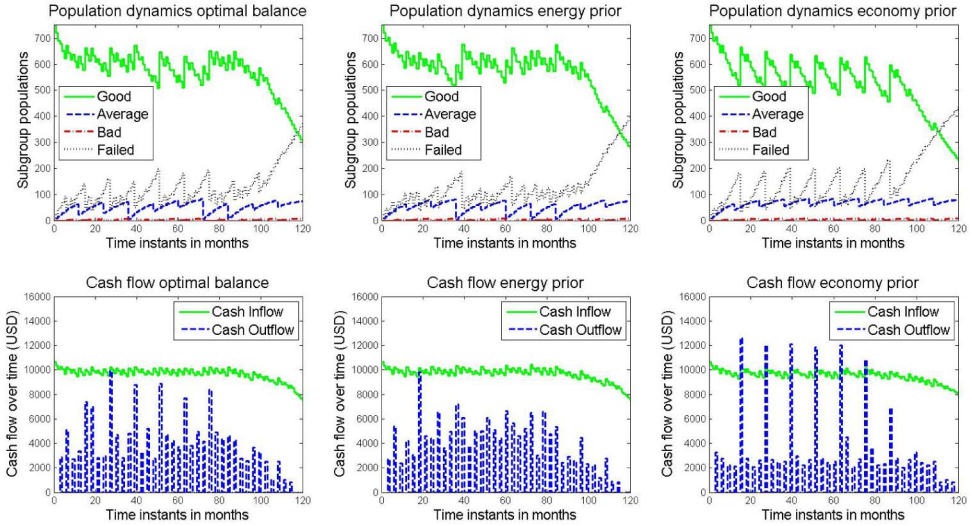

Fig. 4. Performances of the three optimal cases. Both the population dynamics and the cash flows are illustrated.

and failed items are restored without taking the budget limit into account. This may be infeasible in some cases.

The uncertainties in the building context can be resulted from sampling errors, the limited accuracy of population dynamics models, random human behaviors, environmental factors, and stochastic reliability performances [25]. All these resources make the uncertainties very complicated. Therefore, the uncertainties in our system are represented by a series of bounded random noises up to $\pm 5\%$ of the state variables.

The solutions in the three optimal cases manifest satisfying performances in comparison with the full maintenance policy. The energy saving amounts are very close to the full maintenance solution, while the IRR and NPV values become larger and the payback periods are reduced. The maintenance investments are kept within the budget limit and much smaller than the full maintenance cost. All the illustrated performance characteristics in Table III are the mean values of ten-run results with uncertainties. The effectiveness of the present MPC-based approach is thereby verified. The tradeoff between the savings and the IRR can be observed between the energy prior and economy prior. Fig. 4 demonstrates the respective performances in each case. In addition to the population dynamics, the cash flows are also illustrated. We believe that the cash inflow can indicate the benefit of the retrofitting project while the cash outflow reflects the magnitude of control inputs, i.e., the maintenance intensities. Fig. 5 demonstrates the energy saving dynamics in different cases. The black solid line indicates the ideal energy savings without deterioration, which cannot be achieved in practice. The rest four curves, respectively, represent the energy savings in the full maintenance case and the three optimal maintenance cases.

In Table III and Fig. 4, the magnitude of difference is limited. The reason is that in our case study, the government is the owner and the user of the retrofitted building. It is possible to consider the cost savings as a part of the cash inflow. The more the energy savings are achieved, the more the cash inflow can be obtained. As a result, the energy saving objective plays a very important role in the MPO problem. However, when various stakeholders are involved, striking the balance between different interests remains an open problem for the current approach. This issue will be studied in relative extensions.

Fig. 6 compares the performances of both the DE algorithms with the BNFO method and the classical method, where the solid curve indicates the BNFO method and the dashed curve

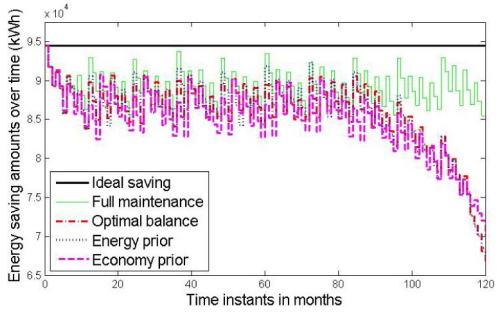

Fig. 5. Energy saving dynamics over the sustainability period in all cases.

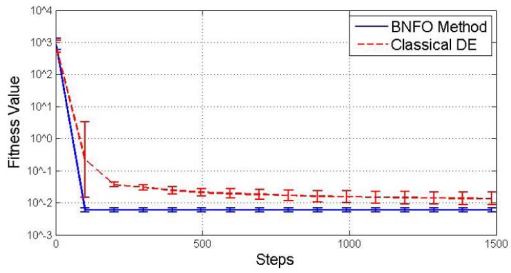

Fig. 6. Convergence of the DE algorithm with the BNFO method and the classical DE algorithm.

indicates the conventional DE algorithm. The logarithmic coordinate is applied to the y-axis for the sake of clearer demonstration. The performances are the mean result over ten runs with the standard errors. As the global optima of minimization problem (15) is unknown in this case study, the local minima is reached as a satisfying solution. In Fig. 6, the solid curve decreases faster than the dashed curve and stops at a smaller fitness value at the end. This illustrates the better convergence and accuracy of the BNFO method.

V. Conclusion

In this brief, the MSS model is employed to formulate the MPO involving both the PM and the CM in a building energy efficiency retrofitting project. For simplicity, the retrofitted items are assumed to be categorized into several homogenous groups, in which each can be divided into several subgroups corresponding to different working states of the items within the homogeneous group. The population dynamics then follows the state transition of the item. During operation, the items deteriorate to worse working states and can be restored to better working states by maintenance actions. The item group therefore manifests a substantial magnitude of population and performance dynamics under the impacts of multilevel deterioration and multiple types of maintenance actions. In this way, the MPO incorporating the MSS model is cast into an optimal control problem. An MPC approach taking into account the history performances is employed and solved by an improved DE algorithm with the BNFO method. From the simulation results of the case study, the effectiveness of the present approach is illustrated, where the long-term energy saving and the economy of the project are maximized with limited budget under the impacts of the uncertainties, as opposed to the expensive full maintenance strategy.

References

[1] X. Xia and J. Zhang, "Mathematical description for the measurement and verification of energy efficiency improvement," *Appl. Energy*, vol. 111, pp. 247–256, Nov. 2013.
[2] B. Wang, X. Xia, and J. Zhang, "A multi-objective optimization model for the life-cycle cost analysis and retrofitting planning of buildings," *Energy Buildings*, vol. 77, pp. 227–235, Jul. 2014.
[3] X. Ye, X. Xia, L. Zhang, and B. Zhu, "Optimal maintenance planning for sustainable energy efficiency lighting retrofit projects by a control system approach," *Control Eng. Pract.*, vol. 37, pp. 1–10, Apr. 2015.
[4] B. Wang and X. Xia, "Optimal maintenance planning for building energy efficiency retrofitting from optimization and control system perspectives," *Energy Buildings*, vol. 96, pp. 299–308, Jun. 2015.
[5] J. Yan and D. Hua, "Energy consumption modeling for machine tools after preventive maintenance," in *Proc. IEEE Int. Conf. Ind. Eng. Eng. Manage. (IEEM)*, Dec. 2010, pp. 2201–2205.
[6] M. B. Yildirim and F. G. Nezami, "Integrated maintenance and production planning with energy consumption and minimal repair," *Int. J. Adv. Manuf. Technol.*, vol. 74, no. 9, pp. 1419–1430, 2014.
[7] A. Lisnianski, I. Frenkel, and Y. Ding, *Multi-State System Reliability Analysis and Optimization for Engineers and Industrial Managers*. London, U.K.: Springer, 2010.
[8] Y. Liu and H.-Z. Huang, "Optimal replacement policy for multi-state system under imperfect maintenance," *IEEE Trans. Rel.*, vol. 59, no. 3, pp. 483–495, Sep. 2010.
[9] M. D. Le and C. M. Tan, "Optimal maintenance strategy of deteriorating system under imperfect maintenance and inspection using mixed inspection scheduling," *Rel. Eng. Syst. Safety*, vol. 113, pp. 21–29, May 2013.
[10] E. K. Boukas and Z. K. Liu, "Production and maintenance control for manufacturing systems," *IEEE Trans. Autom. Control*, vol. 46, no. 9, pp. 1455–1460, Sep. 2001.
[11] X. Xia, J. Zhang, and A. Elaiw, "An application of model predictive control to the dynamic economic dispatch of power generation," *Control Eng. Pract.*, vol. 19, no. 6, pp. 638–648, 2011.
[12] J. Zhang and X. Xia, "A model predictive control approach to the periodic implementation of the solutions of the optimal dynamic resource allocation problem," *Automatica*, vol. 47, no. 2, pp. 358–362, 2011.
[13] D. Q. Mayne, J. B. Rawlings, C. V. Rao, and P. O. M. Scokaert, "Constrained model predictive control: Stability and optimality," *Automatica*, vol. 36, no. 6, pp. 789–814, 2000.
[14] G. Bianchini, M. Casini, A. Vicino, and D. Zarrilli, "Demand-response in building heating systems: A model predictive control approach," *Appl. Energy*, vol. 168, pp. 159–170, Apr. 2016.
[15] X. Zhuan and X. Xia, "Optimal scheduling and control of heavy haul trains equipped with electronically controlled pneumatic braking systems," *IEEE Trans. Control Syst. Technol.*, vol. 15, no. 6, pp. 1159–1166, Nov. 2007.
[16] D. S. Remer and A. P. Nieto, "A compendium and comparison of 25 project evaluation techniques. Part 1: Net present value and rate of return methods," *Int. J. Prod. Econ.*, vol. 42, no. 1, pp. 79–96, 1995.
[17] Z. Wu and T. W. S. Chow, "Binary neighbourhood field optimisation for unit commitment problems," *IET Generat., Transmiss. Distrib.*, vol. 7, no. 3, pp. 298–308, Mar. 2013.
[18] H. Carstens, X. Xia, and X. Ye, "Improvements to longitudinal clean development mechanism sampling designs for lighting retrofit projects," *Appl. Energy*, vol. 126, pp. 256–265, Aug. 2014.
[19] P. O'Connor and A. Kleyner, *Practical Reliability Engineering*. Chichester, U.K.: Wiley, 2011.
[20] L. Grüne, J. Pannek, M. Seehafer, and K. Worthmann, "Analysis of unconstrained nonlinear MPC schemes with time varying control horizon," *SIAM J. Control Optim.*, vol. 48, no. 8, pp. 4938–4962, 2010.
[21] B. Wang, Z. Wu, B. Zhu, and X. Xia, "Optimal control of maintenance instants and intensities in building energy efficiency retrofitting project," in *Proc. 54th IEEE Conf. Decision Control*, Osaka, Japan, Dec. 2015, pp. 2643–2648.
[22] J. Zhang and A. C. Sanderson, "JADE: Adaptive differential evolution with optional external archive," *IEEE Trans. Evol. Comput.*, vol. 13, no. 5, pp. 945–958, Oct. 2009.
[23] T. A. A. Victoire and A. E. Jeyakumar, "Unit commitment by a tabu-search-based hybrid-optimisation technique," *IEE Proc.-Generat., Transmiss. Distrib.*, vol. 152, no. 4, pp. 563–574, Jul. 2005.
[24] Z. Wu and T. W. S. Chow, "Neighborhood field for cooperative optimization," *Soft Comput.*, vol. 17, no. 5, pp. 819–834, 2013.
[25] Y. Heo, R. Choudhary, and G. A. Augenbroe, "Calibration of building energy models for retrofit analysis under uncertainty," *Energy Buildings*, vol. 47, pp. 550–560, Apr. 2012.